Polymer Chemistry

www.rsc.org/polymers

Volume 2 | Number 5 | May 2011 | Pages 985–1204

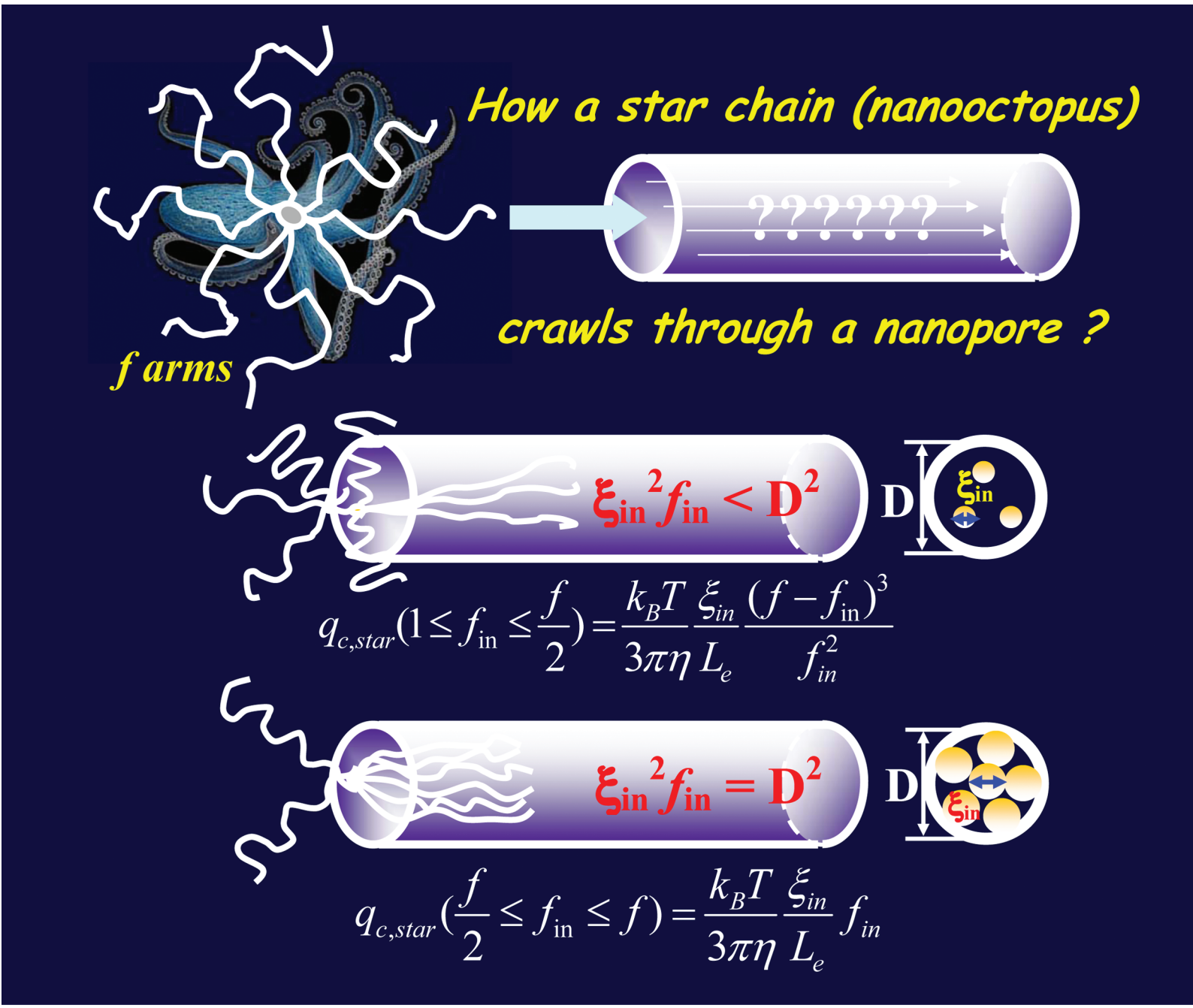

ISSN 1759-9954

RSC Publishing

PAPER
Hui Ge, Stergio Pispas and Chi Wu
How does a star chain (nanooctopus) crawl through a nanopore?

International Year of CHEMISTRY 2011

1759-9954(2011)2:5;1-M

Polymer Chemistry

Dynamic Article Links

Cite this: *Polym. Chem.*, 2011, **2**, 1071

www.rsc.org/polymers

PAPER

How does a star chain (nanooctopus) crawl through a nanopore?

Hui Ge,[a] Stergios Pispas[b] and Chi Wu*[ac]

Received 3rd November 2010, Accepted 20th December 2010
DOI: 10.1039/c0py00361a

The ultrafiltration of star-like polystyrene chains with different arm lengths (L_A) and arm numbers (f) passing through a nanopore (20 nm) under an elongational flow field was investigated in terms of the flow-rate dependent relative retention ($(C_0 - C)/C_0$), where C_0 and C are the polymer concentrations before and after the ultrafiltration. Our results reveal that for a given L_A, the critical flow rate ($q_{c,star}$), below which star chains are blocked, dramatically increases with f; but for a given f, is nearly independent on L_A, contradictory to the previous prediction made by de Gennes and Brochard-Wyart. We have revised their theory in the region $f_{in} < f_{out}$, where f_{in} and f_{out} are the numbers of arms inside and outside the pore, respectively; and also accounted for the effective length of each blob. In the revision, we show that $q_{c,star}$ is indeed independent of L_A but related to both f and f_{in} in two different ways, depending on whether $f_{in} \leq f/2$ or $\geq f/2$. A comparison of our experimental and calculated results reveals that most star chains pass through the nanopores with $f_{in} \sim f/2$. Further study of the temperature dependent $(C_0 - C)/C_0$ of polystyrene in cyclohexane shows that there exists a minimum of $q_{c,star}$ at ~38 °C, close to the theta temperature of polystyrene star chains.

Introduction

De Gennes and Pincus predicted that the critical (minimum) flow rate ($q_{c,1}$) for a linear chain to pass through a nanopore is independent of both the chain length and the pore size,[1,2] *i.e.*, $q_{c,1} = k_BT/(3\pi\eta)$, where k_B, T and η are the Boltzmann constant, the absolute temperature and viscosity, respectively. Our previous study showed that the chain length indeed has no effect on $q_{c,1}$,[3] but $q_{c,1}$ decreases as the pore size increases. In addition, the measured $q_{c,1}$ is ~10–200 time smaller than the predicted ones, depending on the solvent quality and the pore size. Such discrepancies are attributed to an over-simplified assumption in theory; namely, each blob (the subchain confined inside the nanopore) is a hard sphere so that its experienced hydrodynamic force along the flow direction is linearly proportional to the pore diameter (D). In reality, the hydrodynamic force (F_h) experienced by the subchain should be related to its effective length (L_e) along the flow direction, *i.e.*, the integration of all segments inside each subchain along the flow direction, $F_h \propto L_e = \int_0^{l_{c,blob}} \vec{v} dl$, where $\vec{v}$ is the flow velocity, parallel to the central line of the nanopore and $l_{c,blob}$ is the contour length of the subchain. Assuming that the subchain inside each blob is a random Gaussian coil, the average projection of each segment with a length of l_s along the flow direction is $l_s/\sqrt{3}$. Therefore, $L_e = l_{c,blob}/\sqrt{3} = kD^{1/\upsilon} > D$, where k is a scaling constant and $1/2 \leq \upsilon \leq 3/5$, depending on the solvent quality.[4] Clearly, F_h is not a linear function of D so that $q_{c,1}$ should be modified as:[3]

$$q_{c,1} = \frac{k_BT}{3\pi\eta}(D/L_e) = \frac{k_BT}{3\pi\eta}k^{-1}D^{1-\frac{1}{\upsilon}} \quad (1)$$

It is worth noting that on the basis of eqn (1), it is impossible to use the ultrafiltration of linear polymer chains through a nanopore to separate polymer chains with different lengths. The dependence of $q_{c,1}$ on the pore size, was experimentally verified.[3]

In contrast to linear chains, the ultrafiltration of polymers with some complicated structure, such as star and branched configurations, through a nanopore is more intricate. In theory, a regular star polymer with f number of uniform arms joined at a central point might be the simplest case.[5] In 1996, de Gennes and Brochard-Wyart[6,7] formulated how such a star chain passes through a nanopore under an elongational flow field. They showed that the critical (minimum) flow rate ($q_{c,star}$) depends not only on the total number of arms, but also on the number of forward arms (f_{in}) squeezed into the nanopore. In their theory, $q_{c,star}$ is related to the arm length when $f_{in} < f/2$, where they assumed that each forward arm inside the nanopore is fully stretched under the flow field, *i.e.*, by the hydrodynamic force.

Such predictions and their speculated applications have existed for years,[6–8] but have never been experimentally verified. This is partially because this kind of experimental study involves a combination of delicate polymer synthesis and precise physical

[a]*Department of Chemistry, The Chinese University of Hong Kong†, Shatin, N.T., Hong Kong*
[b]*Theoretical and Physical Chemistry Institute, National Hellenic Research Foundation, 48 Vass. Constantinou Avenue, 11635 Athens, Greece*
[c]*The Hefei National laboratory of Physical Science at Microscale, Department of Chemical Physics, The University of Science and Technology of China, Hefei, Anhui, 230026, China*
† *The Hong Kong address should be used for all correspondence.*

characterization. Namely, 1) star polymers should be narrowly distributed in terms of both the arm number and length; 2) the hydrodynamic radius of stars must be larger than the pore diameter, *i.e.*, each arm must be sufficiently long (over 10^3 monomers); and 3) the preparation of a proper nanopore structure so that the flow at its entrance is close to elongational without any rotational component.[7] Recently, using high-vacuum anionic polymerization,[9] we have overcome difficulties in the preparation of star chains with different arm numbers and lengths. Armed with these well-defined star polymers and using our previously established ultrafiltration method, we have finally experimentally studied how star chains pass through a nanopore.

Experimental section

Sample preparations

Polystyrene (PS) linear and star chains (up to 41 arms) with different lengths, as summarized in Table 1, were synthesized using a combination of high-vacuum anionic polymerization and a coupling method using divinylbenzene (DVB).[9–11] Namely, using high-vacuum anionic polymerization, we first prepared narrowly distributed linear PS living chains with an active anionic end by initiating styrene (St, from Aldrich) with n-butyllithium (n-BuLi, 1.5M in cyclohexane, from Aldrich) in cyclohexane at ~30 °C. Furthermore, these linear chains are coupled together to form star chains when a required amount of DVB molecules were added into the solution of living polystyl anions. The ratio of [DVB] : [anions] was kept at 0.7 : 1. All the chemicals were purified before the polymerization. The details can be found elsewhere.[9,11] The coupling reaction between linear polystyl anions and DVB was lasted for 1–7 days, depending on the arm length. The longer the arm length was, the longer the coupling reaction time would be. Further addition of the same amount of DVB resulted in star chains with more arms. Such a step-by-step addition of DVB finally led to a series of star chains with different arm numbers but an identical arm length, as shown in Fig. 1.[10]

Note that such prepared star chains are normally broadly distributed in the arm number. Therefore, we have to further fractionate them by the following procedure;[12] 1) dissolving these star chains in 1,4-dioxane at 80 °C with a concentration of 0.03 g mL^{-1}; 2) adding ethanol dropwise until the solution just became slightly milky; 3) letting the solution stand at the room temperature for few weeks so that a small fraction of star chains with the highest number of arms precipitated out of the solution; and 4) repeating steps 2 and 3 to obtain narrowly distributed star chains

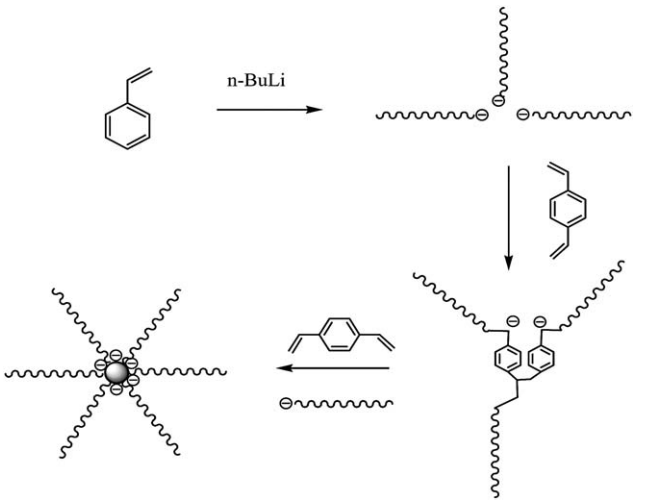

Fig. 1 Schematic of the synthesis of star chains with different arm numbers but an identical arm length using anionic polymerization and the DVB coupling method.

with different arms. The 3-arm star chains ($M_{w\_arm} = 2.1 \times 10^5$ g mol^{-1}, $M_w/M_n = 1.08$) was previously synthesized by using chlorosilane as the coupling agent.[9] The weight-average molar mass (M_w) and polydispersity index (M_w/M_n) of such obtained star chains were characterized by laser light scattering, also as summarized in Table 1.

Laser light scattering (LLS)

A modified commercial LLS spectrometer (ALV/DLS/SLS-5022F) equipped with a multi-τ digital time correlator (ALV5000) and a cylindrical 22 mW UNIPHASE He–Ne laser ($\lambda_0 = 632$ nm) was used. The incident beam was vertically polarized with respect to the scattering plane. The details of the LLS instrumentation and theory can be found elsewhere.[13] Briefly, in static LLS, the excess absolute time-averaged scattered light intensity, known as the excess Rayleigh ratio $R_{vv}(\theta)$, of a dilute polymer solution at concentration C (g mL^{-1}) is related to the weight average molar mass M_w, the root-mean square radius of gyration $<R_g^2>^{1/2}$, and the scattering vector k_s as

$$\frac{KC}{R_{vv}(\theta)} \approx \frac{1}{M_w}\left(1 + \frac{1}{3}<R_g^2> k_s^2\right) + 2A_2C \qquad (2)$$

where $K = 4\pi^2 n^2 (dn/dC)^2/(N_A\lambda_0^4)$ and $k_s = (4\pi n/\lambda_0)\sin(\theta/2)$ with N_A, dn/dC, n, θ and λ_0 being the Avogadro number, the specific

Table 1 Arm number (f), length ($M_{w,arm}$), weight molar mass ($M_{w,star}$), polydispersity index (M_w/M_n) and average hydrodynamic radius ($<R_h>$) of polystyrene star and linear chains in toluene[a]

Code	f	$M_{w,arm}$/(g mol^{-1})	$M_{w,star}$/(g mol^{-1})	M_w/M_n	$<R_h>$/nm
Star-41	41	2.10×10^5	8.61×10^6	1.20	61
Star-6A	6	1.30×10^5	7.80×10^5	1.18	28
Star-6B	6	2.10×10^5	1.26×10^6	1.20	41
Star-6C	6	3.50×10^5	2.10×10^6	1.20	56
Star-3	3	2.10×10^5	6.30×10^5	1.08	32
Star-2 linear chain	2	2.95×10^5	5.90×10^5	1.01	22

[a] Note that relative errors of M_w and $<R_h>$ are 5% and 2%, respectively.

refractive index increment, the solvent refractive index, the scattering angle and the wavelength of the light in vacuum, respectively; and A_2 is the second virial coefficient. For polystyrene in cyclohexane at 34.5 °C and in toluene at 25 °C, $dn/dC = 0.171$ and 0.109 mL g^{-1}, respectively. In dynamic LLS, the intensity-intensity time correlation function ($G^{(2)}(\tau)$) of each polymer solution was measured before and after the ultrafiltration. $G^{(2)}(\tau)$ is related to the normalized field-field autocorrelation function $|g^{(1)}(\tau)|$. The Laplace inversion of each $g^{(1)}(\tau)$ leads to a line-width distribution $G(\Gamma)$ that can be further converted to a hydrodynamic radius distribution $f(R_h)$ by using the Stokes-Einstein equation.[13,14]

Ultrafiltration

In our ultrafiltration experiments, a double layer membrane filter (Whatman, Anotop 10) was used. The top and bottom layers contain an equal number of 200 nm and 20 nm cylindrical pores, respectively; *i.e.*, each large pore is on top of a small pore. Such a structure prevents any possible interference of the flow fields generated by different small pores at their entrances. In each solution, we added a certain amount of short linear chains with a size smaller than the pore diameter. These short linear chains will pass through the nanopore even without any flow so they served as an internal standard. The concentrations of large star and short linear chains (C_L and C_S) are properly chosen so that $<I_L>/<I_S> = C_L M_L / C_S M_S \sim 1$, where M_L and M_S are the molar masses of large star and short linear chains, respectively. Note that in dynamic LLS, $<I_L>/<I_S>$ equals the area ratio of their corresponding peaks in $G(\Gamma)$. Since the nanopore has no retention on short linear chains, the decrease of $<I_L>/<I_S>$ must be related to the retention of large star chains. On the other hand, in static LLS, we can measure the total time-average scattered light intensity ($<I_{tot}> = <I_L> + <I_S>$). A combination of static and dynamic LLS results enables us to determine $<I_L>$ and $<I_S>$ and then the relative retention $[(C_0 - C)/C_0]$ of larger star chains under different flow rates (q).[15] In each ultrafiltration experiment, the solution temperature and q were controlled by an incubator (Stuart Scientific, S160D) (± 0.1 °C) and a syringe pump (Harvard Apparatus, PHD 2000), respectively.

Result and discussion

Fig. 2 shows the flow rate (q) dependent relative retention of 6-arm star chains with different arm lengths in toluene. There is no obvious difference in "$[(C_0 - C)/C_0]$ *vs.* q" among these different 6-arm star chains. As discussed in the introduction, no arm-length dependence of $q_{c,star}$ should only occur in the symmetrical mode;[6] namely, $f_{in} = f/2$. It has to be stated that de Gennes and Brochard-Wyart[6] assumed that when $1 \leq f_{in} < f/2$, each arm inside the nanopore is fully stretched so that its effective length along the flow direction is related to the contour length of each arm. In this way, star chains with shorter arms require a higher flow rate to pull the backward f_{out} arms through the nanopore because the hydrodynamic force on each arm F_h is proportional to both the arm length and the flow rate. Apparently, if de Gennes and Brochard-Wyart were right, Fig. 2 would indicate that these 6-arm star chains would only pass through the nanopore *via* the symmetrical mode, *i.e.*, $f_{in} = f/2$.

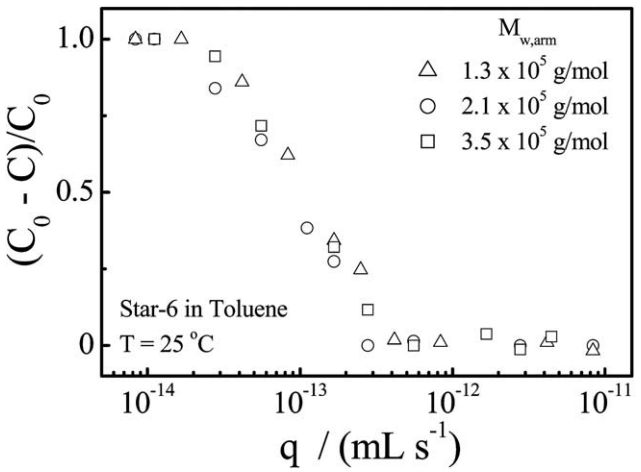

Fig. 2 Flow rate (q) dependence of relative retention $[(C_0 - C)/C_0]$ of star chains with six arms but different arm lengths in toluene, where C_0 and C are the polymer concentrations before and after the ultrafiltration.

Fig. 3 shows that the relative retention of star chains decreases as the flow rate increases. The change is apparently not as abrupt as the first-order coil-to-stretch transition of linear polymer chains observed before.[3,15] It should be noted that here the x-axis is in a logarithmic scale. The transition is actually sharp except for star chains with 41 arms. For Star-41, f_{in} might vary in the range 1–41 and each f_{in} leads to one different $q_{c,star}$, explaining why the change of " relative retention *vs.* q" is not as sharp as those for Star-6 and Star-3 with the same arm length.

Fig. 4 shows a better view of a typical variation of the relative retention with q for Star-41, where we define two critical flow rates ($q_{c,star,s}$ and $q_{c,star,p}$) marked the starting and peaking positions of the relative retention. For Star-41, $q_{c,star,s} = 2.40 \times 10^{-12}$ and $q_{c,star,p} = 5.14 \times 10^{-13}$ mL s^{-1}. These measured critical flow rates are very different from those predicted by de Gennes and Brochard-Wyart.[6] A combination of our experimental

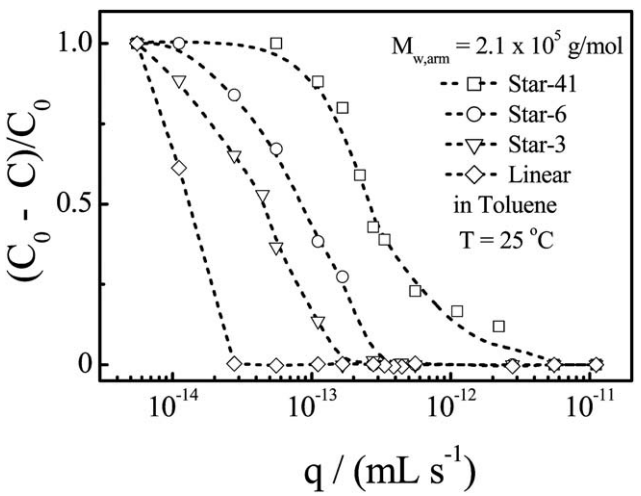

Fig. 3 Flow rate (q) dependence of relative retention $[(C_0 - C)/C_0]$ of star chains with different arm numbers but an identical arm length in toluene, where the weight-average molar mass ($M_{w,arm}$) of each arm is 2.1×10^5 g mol^{-1}.

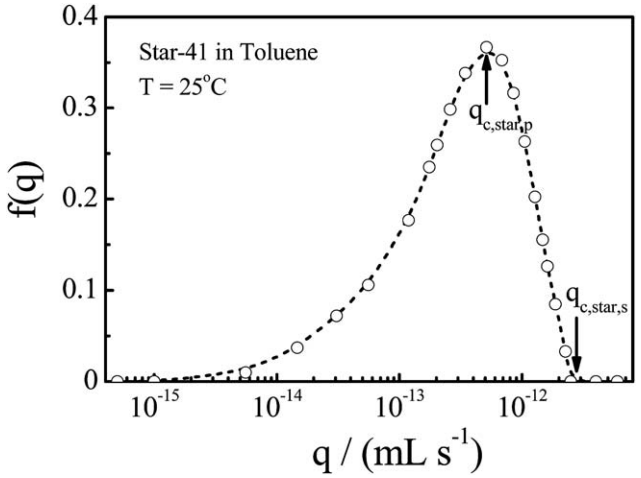

Fig. 4 Differentiation of relative retention to flow rate, $d[(C_0 - C)/C_0]/dq$, for star chains with 41 arms, where $q_{c,star,s}$ and $q_{c,star,p}$ define the starting and peaking points of retention, respectively.

results in Fig. 2 and 3 forces us to rethink whether there is something missing/improper in their assumptions and theoretical treatments presented for a long time but never having been seriously tested.

Fig. 5 schematically illustrates two different paths: $1 \le f_{in} \le f/2$ and $f/2 \le f_{in} \le f$, depending on whether more arms are forward or backward when each star chain enters the nanopore. First, let us consider the translocation without any flow. If f_{in} arms are forward and fill up the nanopore and each arm inside is made of n_b blobs and each blob has a diameter of ξ_{in}, we have $\xi_{in}^2 f_{in} = D^2$ or $\xi_{in} = D/f_{in}^{1/2}$, as shown in Fig. 5. Thermodynamically, the energy and force to confine each blob is k_BT and k_BT/ξ_{in}, respectively, so that the total confinement energy and force (E_c and F_c) should be $k_BTn_bf_{in}$ and $(k_BT/\xi_{in})n_bf_{in}$. Assuming that each arm (blob) contains N_{arm} (N_b) segments, $n_b = N_{arm}/N_b$ and $\xi_{in} = kN_b^{\nu}$. Putting everything together, we have $E_c = k_BTN_{arm}(k/D)^{1/\nu}f_{in}^{(1+1/2\nu)}$ for f_{in} forward arms. If the entire star chain enters the nanopore, the total confinement energy should also include those backward $(f - f_{in})$ arms, *i.e.*, $E_{total} = k_BTN_{arm}(k/D)^{1/\nu}[f_{in}^{(1+1/2\nu)} + (f - f_{in})^{(1+1/2\nu)}]$. The differentiation $dE_{total}/df_{in} = 0$ leads to that the minimum of E_{total} occurs at $f_{in} = f/2$.

Second, let us consider the translocation under a flow. When $f/2 \le f_{in} \le f$, we only need to consider under which flow rate f_{in} arms can enter the nanopore with a diameter (D), and do not need to worry about the backward arms because $f_{out} = f - f_{in} <$ f_{in}. The hydrodynamic force on each blob inside is $3\pi\eta l_e(q/D^2)$ and the total hydrodynamic force (F_h) is $3\pi\eta l_e(q/D^2)n_bf_{in}$, where l_e is the effective length of each blob along the flow direction. The condition of $F_h = F_c$ leads to the critical flow rate for $f/2 \le f_{in} \le f$,

$$q_{c,star}\left(\frac{f}{2} \le f_{in} \le f\right) = \frac{k_BT}{3\pi\eta} f_{in} \frac{\xi_{in}}{l_e} \tag{3}$$

An attentive reader might find that in the above discussion we only need to consider under which flow rate the first blobs of f_{in} forward arms can enter the nanopore because the second and remaining blobs of each arm just follow its first blob. When $1 \le f_{in} \le f/2$, we have to consider how many number of arms are outside of the nanopore, as shown in Fig. 5. Obviously, $q_{c,star}$ calculated in eqn (3) can only pull f_{in} arms in, not sufficient to pull f_{out} arms into the nanopore because $f_{out} > f_{in}$. Therefore, one has to increase q to stretch each forward arm inside the nanopore further, *i.e.*, decreases ξ_{in} at the same time. In this way, $\xi_{in}^2 f_{in}$ becomes smaller than D^2, as also shown in Fig. 5. The decrease of ξ_{in} leads to the increase of the force required to confine each blob. Finally, when $3\pi\eta \frac{q}{D^2} l_e f_{in} = \frac{k_BT}{\xi_{in}} f_{in} = \frac{k_BT}{\xi_{out}} f_{out}$, the hydrodynamic force is just sufficient to pull the outside backward f_{out} arms into and through the nanopore, wherein $\xi_{out}^2 f_{out} = D^2$, *i.e.*, the nanopore is just filled with f_{out} number of arms. Therefore, we have

$$q_{c,star}\left(1 \le f_{in} \le \frac{f}{2}\right) = \frac{k_BT}{3\pi\eta} \frac{f_{out}^3}{f_{in}^2} \frac{\xi_{in}}{l_e} \tag{4}$$

If each blob is considered as a hard sphere, *i.e.*, $l_e = \xi_{in}$, eqn (3) and (4) become

$$q_{c,star}\left(\frac{f}{2} \le f_{in} \le f\right) = \frac{k_BT}{3\pi\eta} f_{in} \tag{5a}$$

$$q_{c,star}\left(1 \le f_{in} \le \frac{f}{2}\right) = \frac{k_BT}{3\pi\eta} \frac{(f - f_{in})^3}{f_{in}^2} \tag{5b}$$

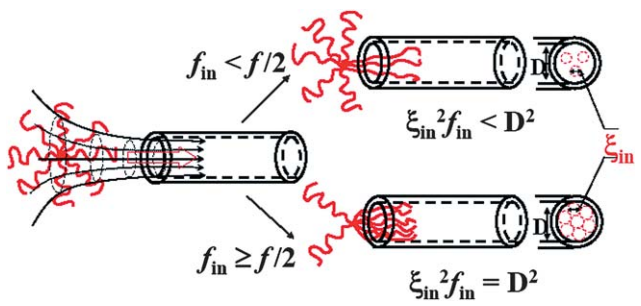

Fig. 5 Schematic of how a star chain enters a nanopore under two different situations; namely, $f \ge f_{in} \ge f/2$ and $f/2 \ge f_{in} \ge 1$.

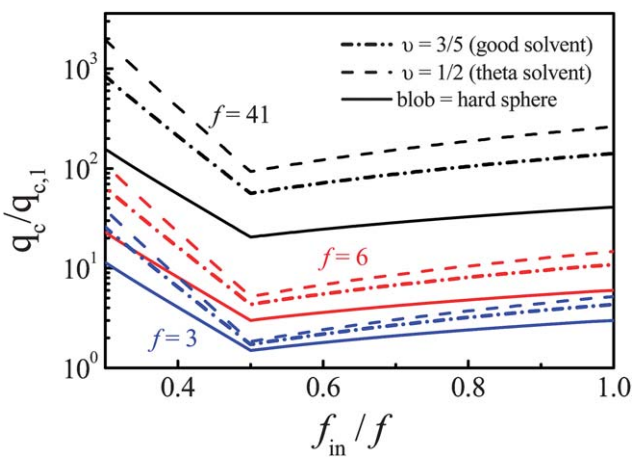

Fig. 6 Forward arm number (f_{in}) dependence of reduced critical flow rate ($q_{c,star}/q_{c,1}$) of star chains with different arm numbers but an identical arm length, calculated on the basis of eqn (5) and (6), respectively.

Our revised formulas reveal that $q_{c,star}$ is independent of the arm length no matter whether f_{in} is larger or smaller than $f/2$. Note that eqn (5a) is identical to that in ref. 6 in which de Gennes and Brochard-Wyart mistakenly wrote f_{in}^2 instead of f_{in}.

The continuous lines in Fig. 6 shows how $q_{c,star}$ changes with f_{in} for star chains with different arm numbers on the basis of eqn (5a) and (5b). Note that $q_{c,star}$ linearly increases with f_{in} in the range $f/2 \leq f_{in} \leq f$, but dramatically increases as f_{in} decreases when $f_{in} \ll f/2$. The minimum is located at $f_{in} = f/2$, different from the optimal f_{in} predicted by de Gennes and Brochard-Wyart.[6] Physically, this is reasonable because the decrease of f_{in} reduces the overall hydrodynamic force on the forward arms inside the nanopore, and at the same time, increases the force required to confine those backward arms still outside the nanopore. As discussed in the section of Introduction, for linear chains, we can treat the subchain inside each blob as a random Gaussian coil so that $l_e = k\xi_{in}^{1/\upsilon}$. Therefore, eqn (5a) and (5b) can be rewritten as

$$q_c\left(\frac{f}{2} \leq f_{in} \leq f\right) = q_{c,1} f_{in}^{\frac{1}{2}(1+\frac{1}{\upsilon})} \quad (6a)$$

$$q_c\left(1 \leq f_{in} \leq \frac{f}{2}\right) = q_{c,1} \frac{(f - f_{in})^{\frac{3}{2}(1+\frac{1}{\upsilon})}}{f_{in}^{1+\frac{1}{\upsilon}}} \quad (6b)$$

where $q_{c,1}$ is defined by eqn (1). Eqn (6) also shows that $q_{c,star}$ is only related to both f_{in} and f and independent on the arm length, agreeing with our experimental results in Fig. 2. Note that linear chains are a special kind of star chains with $f = 2$ and $f_{in} = 1$. Under this special condition, $q_{c,star}$ in eqn (6), as expected, returns to $q_{c,1}$. Fig. 6 also shows how $q_{c,star}$ vary with f_{in} for each given f and υ. Further, we can estimate f_{in} from our measured values of $q_{c,star}/q_{c,1}$ on the basis of eqn (5) and 6. The results are summarized in Table 2.

For Star-41, $q_{c,star,p}/q_{c,1}$ is around 26, not too far away from the minimum point ($f_{in} = f/2$) calculated from eqn (5), but lower than that calculated from eqn (6). The difference between eqn (5) and (6) is whether we should treat each blob as a hard sphere. When a half number of arms of a Star-41 chain is squeezed into a nanopore with a diameter of 20 nm, ξ_{in} is only 4–5 nm so that each arm should be highly stretched. Note that the estimated diameter of a polystyrene chain is ~1.2 nm. Therefore, each blob can be viewed as a hard ball filled with the segments of the subchain without draining, explaining why its $q_{c,star,p}/q_{c,1}$ is close to those calculated from eqn (5). Also note that for Star-41, f_{in} is larger than 13, which is understandable because $q_{c,star}$ increases sharply when f_{in} is low for star chains with a high number of arms.

On the other hand, for Star-6 and Star-3, $q_{c,star,p}/q_{c,1} = 6.3$ and 2.8 respectively, slightly higher than the minimum points (3 and 1–2) calculated based on eqn (5), but more close to 4 and 2 estimated from eqn (6). It indicates that for star chains with a lower number of arms, eqn (6) is a better choice because the subchain inside each blob is much less confined; namely, it is not necessary to fully stretch each arm to pull the outside backward arms into the nanopore. Also note that a comparison of experimentally measured values of $q_{c,star}/q_{c,1}$ and eqn (6) shows that $2 \leq f_{in}$(Star-6) ≤ 6 and $1 \leq f_{in}$(Star-3) ≤ 3, revealing that star chains with a lower number of arms can enter the nanopore in different ways, even if its mostly preferred path is $f_{in} \sim f/2$.

Further, we studied the effect of the arm conformation on $q_{c,star}$ by dissolving polystyrene star chains in cyclohexane in which each arm contracts as the solution temperature decreases below its theta temperature (~34.5 °C), as shown in Fig. 7. It should be noted that both the average radius of gyration ($<R_g>$) and hydrodynamic radius ($<R_h>$) of Star-41 chains decrease with the solution temperature, but the change is much smaller than that of linear PS chains within the same temperature range,[5,16] presumably because 41 arms are crowed within a small space and the excluded volume prevents their collapse even in a poor solvent (lower temperatures). It should be noted that in the temperature range studied there is no change in the scattered light intensity, implying that there is no interchain association.

It has been previously suggested that the temperature at which q_c reaches its minimum could be attributed to the true theta solvent,[3] which was based of a reasonable assumption that polymer chains at the theta solvent are softest and mostly deformable, *i.e.*, in a good solvent, the chain is highly swollen so that a stronger hydrodynamic force is required to stretch it into a string of blobs and confine each blob inside the nanopore due to its entropic elasticity; while in a poor solvent, the segment-segment attraction is stronger than the segment-solvent interaction so that a stronger hydrodynamic force is needed to overcome the enthalpy-originated force.

Table 2 Experimental determined values of reduced critical flow rate ($q_{c,star}/q_{c,1}$) and corresponding f_{in} calculated on the basis of eqn (5) and (6), where $q_{c,1}$ is the critical flow rate for linear chains

		f_{in}	
Code	Measured $q_{c,star}/q_{c,1}$	eqn (5a) and (5b)	eqn (6a) and (6b)
Star-41	26.5–128.9	13–41	18–38
Star-6	6.3–21.8	2–6	2–6
Star-3	2.8–14.4	1–3	1–3

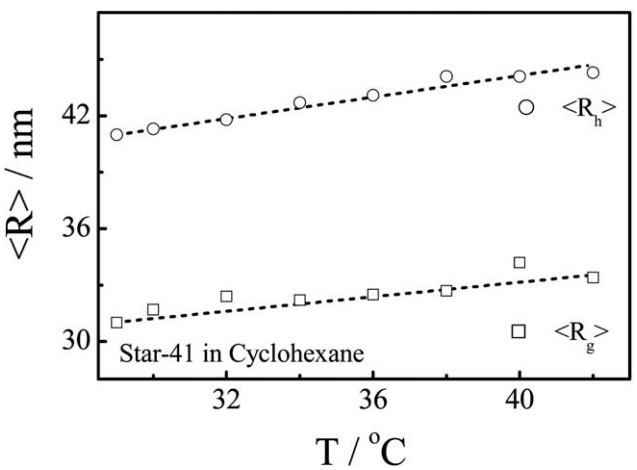

Fig. 7 Solution temperature dependence of average radius of gyration ($<R_g>$) and average hydrodynamic radius ($<R_h>$) of star chains with 41 arms in cyclohexane.

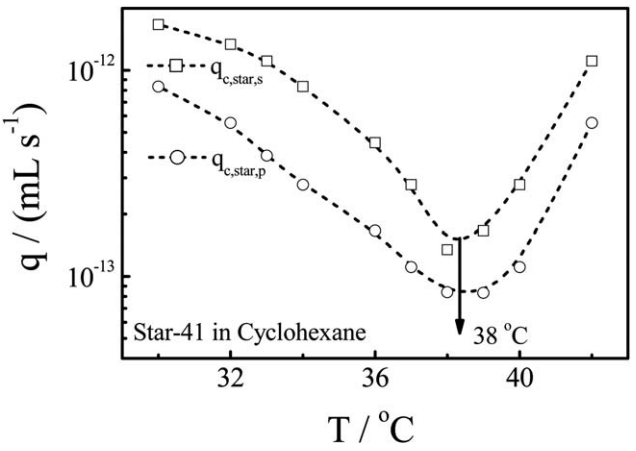

Fig. 8 Solution temperature dependence of $q_{c,star,s}$ and $q_{c,star,p}$ of star chains with 41 arms in cyclohexane.

Fig. 8 shows the temperature dependence of $q_{c,star,s}$ and $q_{c,star,p}$ of Star-41 in cyclohexane at different flow rates. Despite that there is not much change in both $<R_g>$ and $<R_h>$, $q_{c,star}$ varies a lot in the same temperature range because the collapse of a star chain at lower temperatures is hindered by the excluded volumes of different arms but the hydrodynamic force experienced inside the nanopore is related to the properties of individual arms, similar to that of linear chains free in solution. For Star-41, the minimum of q_c is located at ~38 °C, few degrees higher than that of linear polystyrene chains.[17] Such a difference has been previously reported for star and branched chains, especially when the arm number is high and the arm or branch is long,[18–20] presumably because the star and branching configurations increase the distance between segments so that the inter-segment attraction becomes stronger.

Conclusion

The ultrafiltration of star chains with different arm numbers and lengths reveals that the critical (minimum) flow rate ($q_{c,star}$), at which the chains start to pass through a nanopore, is independent of the arm length but strongly influenced by the number of total arms and forward arms that initially enter the nanopore (f and f_{in}), contrary to a previous prediction made by de Gennes and Brochard-Wyart in the 90s in which there exists an optimum number of f_{in} between 1 and $f/2$. Our revision of their theory shows that such a discrepancy is attributed to their assumption that each forward arm inside the nanopore is fully stretched by the flow when $f_{in} < f_{out}$. In our revised formulation, the passing of a star chain through a nanopore depends on whether $f_{in} \leq f/2$ or $f_{in} \geq f/2$. In the case of $f_{in} \geq f/2$, $q_{c,star}$ linearly increases with f_{in}, fairly slowly; but when $f_{in} \leq f/2$, $q_{c,star} \sim (f - f_{in})^3/f_{in}^2$, it dramatically drops as f_{in} increases, especially when f is high. The minimum of $q_{c,star}$ is exactly located at $f_{in} = f/2$, independent of the arm number and length. Our experimental results confirm that most of star chains indeed pass through the nanopore with f_{in} around $f/2$, especially when f is high, not involving the fully stretched forward arms. Further, our study of star chains with 41 arms in cyclohexane at different temperatures reveals that there is a minimum $q_{c,star}$ located at ~38 °C, slightly higher than the theta temperature, which demonstrates that as in the case of linear chains, the ultrafiltration of star chains in a dilute solution through a nanopore provides a better and convenient way to determine the theta temperature. This study has laid a foundation for further applications of using the ultrafiltration to separate and characterize star chains with different arm numbers. Our results also have some implications in the design of non-viral polymeric carriers with different architectures for transporting drugs or genes into or through some organs, such as the kidney and liver.

Acknowledgements

The financial support of the National Natural Scientific Foundation of China Projects (50773077 and 20934005) and the Hong Kong Special Administration Region Earmarked Projects (CUHK4037/07P, 2160331; CUHK4046/08P, 2160365; CUHK4039/08P, 2160361; and CUHK4042/09P, 2160396) is gratefully acknowledged.

References

1 P. G. De Gennes, *J. Chem. Phys.*, 1974, **60**, 5030.
2 P. Pincus, *Macromolecules*, 1976, **9**, 386.
3 H. Ge, F. Jin, J. F. Li and C. Wu, *Macromolecules*, 2009, **42**, 4400.
4 *Polymer Solutions: An Introduction to Physical Properties*, ed. I. Teraoka, John Wiley & Sons, Inc., New York, 2002.
5 M. Daoud and J. P. Cotton, *J. Physique*, 1982, **43**, 531.
6 F. Brochard-Wyart and P. G. De Gennes, *C. R. Acad. Sci., Ser. II*, 1996, **323**, 473.
7 P. G. De Gennes, *Adv. Polym. Sci.*, 1999, **138**, 91.
8 D. M. Meunier and P. B. Smith, *Macromolecules*, 2005, **38**, 5313.
9 N. Hadjichristidis, M. Pitsikalis, S. Pispas and H. Iatrou, *Chem. Rev.*, 2001, **101**, 3747.
10 H. J. Lee, K. Lee and N. Choi, *J. Polym. Sci., Part A: Polym. Chem.*, 2005, **43**, 870.
11 N. Hadjichristidis, H. Iatrou, S. Pispas and M. Pitsikalis, *J. Polym. Sci., Part A: Polym. Chem.*, 2000, **38**, 3211.
12 S. Q. Zhou, S. Y. Fan, S. T. F. Au-yeung and C. Wu, *Polymer*, 1995, **36**, 1341.
13 B. Chu. *Laser Light Scattering*, Academic Press,New York, 2nd edn, 1991.
14 B. J. Berne, R. Pecora. *Dynamic Light Scattering*, Plenum Press, New York, 1976.
15 F. Jin and C. Wu, *Phys. Rev. Lett.*, 2006, **96**, 237801.
16 B. Appelt and G. Meyerhoff, *Macromolecules*, 1980, **13**, 657.
17 B. Chu, Q. Ying and A. Y. Grosberg, *Macromolecules*, 1995, **28**, 180.
18 D. Papanagopoulos and A. Dondos, *Eur. Polym. J.*, 2004, **40**, 2305.
19 F. Ganazzoli and G. Allegra, *Macromolecules*, 1990, **23**, 262.
20 A. Dondos and D. Papanagopoulos, *Polymer*, 1997, **38**, 6255.

